UNIVERSIDAD AUTÓNOMA DE SAN LUIS POTOSÍ

FACULTAD DE CIENCIAS QUÍMICAS

PROGRAMA DE POSGRADO EN BIOPROCESOS

ESTABILIDAD QUÍMICA DE LA β-LACTOSA EN FUNCIÓN DE LA HUMEDAD RELATIVA

TESIS QUE PARA OBTENER EL GRADO DE

MAESTRO EN CIENCIAS EN BIOPROCESOS

PRESENTA:

ING. Edgar Enrique Lara Mota

DIRECTOR DE TESIS:

DRA. Claudia Álvarez Salas

CO-DIRECTOR DE TESIS

DRA. María Zenaida Saavedra Leos

SAN LUIS POTOSÍ, S. L. P. AGOSTO 2021

UNIVERSIDAD AUTÓNOMA DE SAN LUIS POTOSÍ

FACULTAD DE CIENCIAS QUÍMICAS

PROGRAMA DE POSGRADO EN BIOPROCESOS

ESTABILIDAD QUÍMICA DE LA β-LACTOSA EN FUNCIÓN DE LA HUMEDAD RELATIVA

TESIS QUE PARA OBTENER EL GRADO DE:

MAESTRO EN CIENCIAS EN BIOPROCESOS

PRESENTA:

ING. Edgar Enrique Lara Mota

DIRECTOR DE TESIS:
DRA. Claudia Álvarez Salas
CO-DIRECTOR DE TESIS
DRA. María Zenaida Saavedra Leos

SINODALES:

PRESIDENTE:
DRA. Claudia Álvarez Salas _____

SECRETARIO
DRA. María Zenaida Saavedra Leos _____

VOCAL:
DR. Alejandro Rocha Uribe _____

SAN LUIS POTOSÍ, S. L. P. AGOSTO 2021

Proyecto realizado en:

Laboratorio de Investigación de Ingeniería Agroindustrial, de la Facultad de Ingeniería, Universidad Autónoma de San Luis Potosí y en el Laboratorio de Análisis Térmico y Laboratorio de Rayos X del Centro de Investigación en Materiales Avanzados (CIMAV) Unidad Monterrey, Nuevo León, México.

Con financiamiento de:

Consejo Nacional de Ciencias y Tecnología (CONACYT), mediante el proyecto No. 1007834

El programa de Maestría en Ciencias en Bioprocesos de la Universidad Autónoma de San Luis Potosí pertenece al Programa Nacional de Posgrados de Calidad (PNPC) del CONACYT, registro 000588, en el Nivel Maestría (Consolidado).

Número de registro de la beca otorgada por CONACYT: 1007834



Estabilidad química de la β-lactosa en función de la humedad relativa por Edgar Enrique Lara Mota esta obra está bajo una licencia de creative commons reconocimiento-nocomercial-sinobraderivada 4.0 internacional.

AGRADECIMIENTOS ACADÉMICOS

A mis directoras de tesis, la Dra. Claudia Alvarez Salas y la Dra. María Zenaida Saavedra Leos, por la oportunidad de formar parte de su grupo de trabajo. Quiero expresar mi gratitud por todo el apoyo y dedicación durante la realización de mi trabajo, por el tiempo que compartieron conmigo, por cada uno de los momentos en que me guiaron y aconsejaron, para aclarar dudas, pero principalmente me siento agradecido por su confianza. He vivido una gran experiencia durante mi trabajo de maestría y fue en gran medida por la energía que me transmiten, por cultivar en mi el deseo de crecer como persona, así como también, promover mi la inquietud de generar y compartir mis conocimientos con el mundo.

Agradezco al Dr. Alejandro Rocha Uribe por formar parte de mi comité tutorial, por sus atinados comentarios y sugerencias para fortalecer mi proyecto de investigación, de igual manera agradezco por los ánimos brindados para salir adelante y terminar este trabajo a pesar de las circunstancias.

AGRADECIMIENTOS PERSONALES

Dedico el presente trabajo mi familia porque es la piedra angular en mi vida. Agradezco a mis padres por ser los primero en apoyar mis sueños y estar para mi en todo momento, gracias por siempre confiar en mí y alentarme en mis proyectos. Gracias, madre por cuidar siempre de mí, por ser mi principal apoyo, por brindarme tus opiniones y consejos. Gracias, padre por estar siempre ahí, por enseñarme valores y respetar a los demás, eres un ejemplo de que se puede salir adelante sin importar lo que vivas. Ambos han sido mi mayor motivación para ser mejor.

Agradezco a mis hermanos y mis sobrinos por todo su amor, sus palabras de aliento y por darme la certeza de que siempre estarán ahí para apoyarme. Hemos vivido tantas aventuras, siempre riendo y cuidándonos, son mi motivación para ser una persona de bien y un ejemplo para ustedes.

También quiero agradecer a las personas que pude conocer durante esta etapa, he tenido la suerte de convivir con personas grandiosas, he aprendido mucho de ustedes y me llevo gratos recuerdos porque han hecho de esta experiencia una aventura extraordinaria. De manera particular quiero agradecer a mis compañeras de generación Citlalli y Paola, por compartir su tiempo, experiencias y conocimiento. En poco tiempo se ganaron mi confianza, amistad y respeto. Las admiro muchísimo, son personas extraordinarias, de las que te encuentras una vez en la vida, sé que en un futuro cercano serán muy exitosas, les deseo lo mejor siempre y le agradezco a dios por haberlas conocido, siempre estaré para ustedes.

Finalmente quiero agradecer a mis compañeros de licenciatura Diana L., Eduardo, Diana Elizabeth, Iliana, Paloma y Andrés, a pesar de no vernos tan seguido hemos mantenido la buena amistad, les agradezco por siempre alentarme a seguir adelante, son personas maravillosas, fueron los primeros en los que pude confiar y siempre les agradeceré por ello. Especialmente agradezco a Claudia por estar siempre conmigo y por compartir tantas experiencias, lo que hemos vivido ha sido de lo mejor en vida, estoy inmensamente agradecido contigo, te admiro como a nadie más, sé que cumplirás todos tus sueños y estaré ahí contigo apoyándote.

INDICE GENERAL

Abstract ……. 1

Abstract traducido al español ……. 2

Resumen…… 3

Introducción…….. 3

Objetivos…… 5

Materiales y métodos……. 5

1.1 Materiales..... 5

1.2 Preparación de β-lactosa (Lβ)…….. 6

1.3 Isotermas de sorción……... 6

1.4 Caracterización fisicoquímica de Lβ……... 7

1.4.1 Espectroscopia Raman…… 7

1.4.2 Difracción de Rayos X (DRX)……. 7

1.4.3 Microscopia Electrónica de Barrido (SEM)…… 7

1.4.4 Calorimetría Diferencial de Barrido Modulada (MDSC)... 7

Resultados y discusión……..... 8

Conclusiones ……..…… 10

Bibliografía……..…….. 11

Reseña del artículo: Cutting-edge advances on the stability and state diagram of pure β-lactose……. 12

ANEXO: MANUSCRITO ENVIADO……..……. 13

ABSTRACT

A state diagram is a useful tool to visualize the stability limits of a material subjected to different conditions. In this work, the equilibrium state diagram for pure anhydrous beta lactose (Lβ) stability is reported. For this, adsorption isotherms were built at three storage temperatures (15, 25 and 35 ° C) in a wide range of water activity (0.07-0.972). The powders obtained were characterized by Raman spectroscopy, X-ray diffraction (XRD), scanning electron microscopy (SEM), and modulated differential scanning calorimetry (MDSC). The results showed a high stability of Lβ at the storage temperatures, indicating an adsorption similar to the monolayer content. Conversely, the mutarotation process was triggered by the adsorption of water beyond the monolayer content. Under these conditions, the presence of alpha lactose (Lα) was observed. Furthermore, the Tg of the Lβ was determined in the range of -15 to -1.4 °C at the storage conditions. The present work contributes to the study of the stability of Lβ to establish its technological application as a carrier agent or in the microencapsulation of active ingredients.

Keywords: β-lactose stability, lactose mutarotation, equilibrium state diagram, thermal characterization, technological application.

Abstract traducido al español

Un diagrama de estado es una herramienta útil para visualizar los límites de estabilidad de un material sometido a diferentes condiciones. En este trabajo, se informa el diagrama de estado de equilibrio para la estabilidad de la lactosa beta anhidra pura (Lβ). Para ello, se construyeron isotermas de adsorción a tres temperaturas de almacenamiento (15, 25 y 35 ° C) en un amplio rango de actividad del agua (0,07-0,972). Los polvos obtenidos se caracterizaron mediante espectroscopía Raman, difracción de rayos X (XRD), microscopía electrónica de barrido (SEM) y calorimetría diferencial de barrido modulada (MDSC). Los resultados mostraron una alta estabilidad de Lβ a las temperaturas de almacenamiento, lo que indica una adsorción similar al contenido de monocapa. Por el contrario, el proceso de mutarrotación se desencadenó por la adsorción de agua más allá del contenido de monocapa. En estas condiciones, se observó la presencia de alfa lactosa (Lα). Además, la Tg de Lβ se determinó en el intervalo de -15 a -1,4 ° C en las condiciones de almacenamiento. El presente trabajo contribuye al estudio de la estabilidad de Lβ para establecer su aplicación tecnológica como agente portador o en la microencapsulación de principios activos.

Palabras clave: Estabilidad de β-lactosa, mutarrotación de lactosa, diagrama de estado de equilibrio, caracterización térmica, aplicación tecnológica

Resumen

Cutting-edge advances on the stability and state diagram of pure β-lactose

Introducción

La lactosa C12-H22-O11 (β-D-galactopiranosil-D-glucopiranosa) está formada por una molécula de galactosa y otra de glucosa, unidas por un enlace glucosídico β (1,4). Al igual que otros azúcares reductores, la lactosa existe parcialmente como una cadena abierta con un grupo aldehído libre, mediante el cual pueden formar un enlace hemiacetal para formar una estructura cíclica. Con la formación del enlace hemiacetal se genera un nuevo centro quiral, con el cual se da origen a dos tipos de isómeros o anómeros: α o β. Las formas α y β de la lactosa son estereoisómeros que difieren en el arreglo espacial del grupo -OH del carbono anomérico de la molécula de glucosa. En solución, el proceso de transformación entre las formas α y β es denominado mutarrotación y, a temperatura ambiente existen en una proporción aproximada de un 63 % en la forma β y 37 % en la forma α (Fox, 2009). La lactosa se encuentra en estado cristalino, amorfo o en una mezcla de ambos. Con relación a la lactosa amorfa, las moléculas no están organizadas en un patrón regular, predominando las formas esféricas lisas con diferentes tamaños. Por otro lado, en la lactosa cristalina se presenta una estructura bien ordenada, con la forma exacta de un cristal liso bien definido el cual depende de las condiciones de cristalización (Walstra y Jenness, 1984).

La lactosa cristalina se encuentra predominantemente en la forma α-lactosa monohidratada (Lα•H2O, relación molar de agua a lactosa 1:1), pero también puede existir en 3 formas diferentes de anhidrato polimórfico: β-lactosa anhidra (Lβ), α-lactosa anhidra higroscópica inestable (LαH) y α-lactosa anhidra estable (LαS). La forma cristalina que la lactosa pueda adquirir dependerá de las condiciones de proceso y almacenamiento: humedad relativa (HR), la actividad del agua (aw) y la temperatura (Allan et al., 2020). Con relación a la estructura cristalina de la Lα•H2O, cristaliza en forma de celdas monoclínicas, así mismo, las celdas pueden tener diferentes formas dependiendo de la sobresaturación: cuando la sobresaturación es alta se forman

prismas, en cambio, si la sobresaturación es baja se forman cristales en forma de diamante, pirámide o en forma de hacha de guerra o “tomahawk”. Con relación a la estructura cristalina de Lβ, presenta forma de diamante de lados irregulares cuando se cristaliza en agua y prismas con forma de aguja curva cuando se utiliza alcohol en la cristalización (Listiohadi et al. 2005).

β-lactosa anhidra

La industria farmacéutica invierte cantidades considerables de tiempo y dinero en desarrollar y verificar métodos que aseguren la calidad final de sus productos, determinando los componentes y la distribución de estos en la matriz del producto farmacéutico, la cual está constituida por el principio activo o fármaco y los excipientes. La estabilidad de las formulaciones farmacéuticas que utilizan polimorfos de lactosa como excipientes en formas sólidas orales, puede verse afectada por varias razones, entre las más importantes se encuentran: la variación de la cantidad de los diferentes polimorfos, el cambio de la estructura del estado sólido (cristalino, amorfo, amorfo-cristalino) y el apelmazamiento. Estas tres situaciones pueden ocurrir dependiendo de las condiciones de humedad y temperatura durante el procesamiento y almacenaje del producto (Villafuerte, 2007).

La Lβ se forma cristalizando la lactosa en soluciones saturadas de Lα•H2O a temperaturas superiores a 93.5 °C o en soluciones alcohólicas de sales inorgánicas. Por otro lado, se ha demostrado que este polimorfo también puede producirse, a partir de la Lα•H2O, a temperatura ambiente mediante la acción de soluciones deshidratantes, como el metanol, el etanol y la acetona, obteniendo rendimientos superiores al 90%. Sin embargo, independientemente del método utilizado, la obtención de un polvo anomérico completamente libre del otro parece ser un proceso complicado; no obstante, estudios recientes han demostrado que puede obtenerse la β-lactosa totalmente libre del anómero α a temperatura ambiente y, mediante el empleo de soluciones alcohólicas de sales inorgánicas (Lara-Mota et al, 2021).

Existe evidencia de que la composición anomérica afecta las propiedades físicas y funcionales del producto final debido a las diferentes propiedades individuales de estos anómeros. Un ejemplo de la diferencia en las propiedades físicas entre los anómeros es que la solubilidad y la dulzura es diferente siendo mayor para βL que para Lα•H2O. Además, la proporción anomérica en una muestra de polvo afecta indirectamente la fluidez y el comportamiento de compactación del producto debido a cambios en la morfología de la superficie del material cristalizado (Beebe y Gilpin, 1983). Por lo tanto, es importante resaltar que después de una extensa búsqueda en la literatura, este es el primer trabajo dónde se determinan las condiciones de humedad relativa y temperatura para β-lactosa pura, con el propósito de evaluar su estabilidad y conocer si existe una interconversión hacia otros polimorfos.

Objetivos

- Evaluar el efecto de la humedad relativa y la temperatura de almacenamiento sobre β-lactosa mediante la determinación de las isotermas de sorción.
- Caracterizar espectroscópicamente la β-lactosa mediante Espectroscopia Raman (RS) y Difracción de Rayos X (XRD).
- Caracterizar morfológicamente la β-lactosa mediante Microscopía Electrónica de Barrido (SEM).
- Caracterizar térmicamente la β-lactosa mediante Calorimetría Diferencial de Barrido (DSC).

Materiales y métodos

1.1 Materiales

α-lactosa monohidratada, (Lα·H2O, pureza ≥ 99,9%) adquirido de Sigma-Aldrich Chemical Co., metanol (MeOH, grado reactivo ≥ 99,8) de J.T. Baker, hidróxido de sodio (KOH, grado reactivo ≥90%) de Fermont y agua destilada se emplearon como

reactivos para obtener β-lactosa pura. Las sales inorgánicas utilizadas para someter los polvos de lactosa a diferentes condiciones de humedad fueron de la marca Fermont con una pureza ≥90%: hidróxido de sodio (NaOH), acetato de potasio (CH3COOK), cloruro de magnesio (MgCl2), carbonato de potasio (K2CO3), magnesio. Nitrato [Mg (NO3)2], Nitrato de Sodio (NaNO3), Cloruro de Potasio (KCl) y Sulfato de Potasio (K2SO4).

1.2 Preparación de β-lactosa (Lβ)

La obtención del anómero Lβ puro se realizo a partir de las metodologías descritas por Lara-Mota et al. 2021. Se prepararon soluciones metanólicas de KOH en relación 1:10 que contenían 15 g de Lα•H2O, la solución fue sometida a reflujo por dos horas a una temperatura de 65°C y posteriormente se filtró. Adicionalmente, se realizaron lavados de la muestra con una solución metanólicas de HNO3 a una concentración de 0.00014 M hasta ajustar a pH neutro. Las muestras fueron secadas a temperatura ambiente.

1.3 Isotermas de sorción

Las isotermas de sorción se determinaron mediante el método gravimétrico a 15, 25 y 35 °C. Los microambientes utilizados se seleccionaron en un intervalo de a_w de 0.07 a 0.972. Se equilibraron 7 días a cada temperatura, para posteriormente agregar 2g de Lβ a las diferentes condiciones de humedad relativa. Se realizo el pesaje de las muestras cada 24 horas hasta alcanzar peso constante con diferencia ± 0,001 g. Se determino el contenido de humedad de equilibro y los datos obtenidos se ajustaron al modelo matemático propuesto por Guggenheim, Anderson y Boer (GAB) (Ecuación 1).

$$Xe = \frac{XmCKa_w}{(1-Ka_w)(1-Ka_w+CKa_w)} \qquad \text{Ecuación 1}$$

Donde: Xe es el contenido de humedad en el equilibrio (g H_2O/g m.s.), Xm es el contenido de humedad en la monocapa (g H_2O/g m.s.), aw es la actividad de agua, K y C son las constantes del modelo.

1.4 Caracterización fisicoquímica de Lβ

1.4.1 Espectroscopia Raman

La caracterización de Lβ mediante espectroscopia Raman se realizó utilizando un oriba LabRam HR Evolution con un espectrómetro Jobin Yvon y un láser rojo de He-Ne de 633 nm de longitud de onda. Se utilizó un microscopio Olympus BXFM-ILHS con un objetivo de 100x para enfocar el rayo láser en la muestra. Los espectros Raman se recogieron en un rango de 50 a 1500 cm^{-1}.

1.4.2 Difracción de Rayos X (DRX)

El análisis DRX de Lβ se llevó a cabo en un difractómetro D8 Advance ECO (Bruker, Karlsruhe, Alemania) equipado con radiación Cu-K (l = 1.5406 Å) operado a 45 kV. Las muestras se analizaron en un intervalo de 2θ de 5-50 °, con un tamaño de paso de 0,016° y 20s por paso.

1.4.3 Microscopia Electrónica de Barrido (SEM)

Para determinar la morfología de las muestras se utilizó un microscopio electrónico de barrido JSM-7401F (JEOL, Japón) operado a 2 kV. Las muestras de Lβ fueron dispersadas en una película de carbono de doble cara y se cubrieron con una capa de oro mediante para minimizar los efectos de carga.

1.4.4 Calorimetría Diferencial de Barrido Modulada (MDSC)

El análisis térmico de Lβ se realizó en un calorímetro diferencial de barrido modulado (MDSC) modelo Q200, (TA Instruments, Lukens Drive, New Castle, DE), equipado con un sistema de refrigeración RCS90. La temperatura y entalpía se calibró utilizando indio como estándar, mientras que para la capacidad calorífica se utilizó zafiro. Como gas de purga se utilizó nitrógeno grado HPLC con un flujo de 100 ml/min, para generar una atmósfera inerte. Fueron pesados 10 mg de Lβ en celdas de aluminio TzeroTM selladas. Las rampas de calentamiento y enfriamiento del programa térmico se realizaron con una modulación de 40 s, y una amplitud de 1,5 °C. Los termogramas se adquirieron siguiendo el siguiente procedimiento: (i) isotérmico a -50 °C durante 1

minuto, (ii) calentamiento de -50 a 190 °C a 20 °C/min, (iii) isotérmico a 190 °C durante 1 minuto, (iv) enfriamiento de 190 a -50 ° C a 10 ° C/min, (v) calentamiento de -50 a 300 °C a 10 °C / min. El análisis de los termogramas se realizó mediante el software Universal Analysis 2000, versión 4.4A, para determinar la transición vítrea de enfriamiento (TgC) y la transición vítrea de calentamiento (TgH).

Resultados y discusión

La Lβ se mantuvo estable en un amplio intervalo de a_w, independientemente de la temperatura a la que se sometieron las muestras. El contenido de humedad en las muestras fue constante en un intervalo de a_w de 0.07 a 0.742, absorbiendo en promedio 0.07 g H_2O/g m.s. Cuando la a_w fue superior a 0.742 aumentó de manera exponencial la adsorción de agua, en estas condiciones se vio un efecto de la temperatura en el contenido de humedad final, absorbiendo 2.58, 1.25 y 0.55 g H_2O/g m.s., para 15, 25 y 35 °C, respectivamente. Las isotermas de Lβ presentaron la forma tipo III de isotermas, de acuerdo con la clasificación propuesta por Brunauer, Deming, Deming y Teller en 1940. En la tabla 1 se muestras los parámetros ajustados al modelo de GAB.

Tabla 1. Valores de los parámetros ajustados al modelo de GAB para Lβ

Parámetro	Temperatura		
	15 °C	25 °C	35 °C
Xm	0.0387	0.0409	0.0219
C	38098.7591	38093.7514	38093.7514
K	1.0187	0.9987	0.9953
R^2	0.986	0.994	0.995

Después de alcanzar el equilibrio, las muestras de Lβ a las diferentes a_w fueron caracterizadas para evaluar el efecto de la humedad relativa sobre la estabilidad en la estructura cristalina de Lβ. Mediante la técnica de espectroscopia Raman se pudieron observar los modos vibracionales característicos de Lβ en un intervalo de a_w de 0.07 a 0.742, sin importar la temperatura a la cual fueron almacenadas las muestras, las

vibraciones se presentaron como un doble pico a 357 cm^{-1} y una doble vibración de baja intensidad a 1100 cm^{-1}. Para valores de a_w por arriba de 0.742, se presentaron vibraciones de alta intensidad a longitudes de onda de 357 y 1086 cm^{-1} correspondientes a Lα•H2O. Los resultados obtenidos de DRX mostraron las difracciones características para Lβ a las tres temperaturas evaluadas, en un intervalo de a_w de 0.07 a 0.742, las difracciones se presentaron en un ángulo 2θ a 10.5, 19 y 21°, a partir de la a_w de 0.742, las muestras presentaron las difracciones distintivas de Lα•H2O. El estudio de las muestras mediante SEM confirmo los resultados obtenidos a partir de espectroscopia Raman y DRX, se observa en las micrografías que para el intervalo de a_w de 0.07 a 0.742, sin importar la temperatura evaluada, la morfología de Lβ se conserva con forma de prima de tipo aguja curvo y para valores de a_w superiores a 0.742, la morfología de las muestras cambio por partículas de forma irregular correspondientes a Lα•H2O. Estos resultados indican que el punto límite de estabilidad para Lβ se observa a valores de a_w por arriba de 0.742, cuando la a_w supera este valor la molécula de Lβ absorbe una mayor cantidad de agua, favoreciendo el proceso de mutarrotación, así como la interconversión del anómero Lβ a Lα•H2O, este proceso no solo afecta la composición química de la molécula, sino que también tiene un efecto en la morfología de las partículas.

El análisis de Lβ mediante la técnica de MDCS se utilizo para determinar los eventos térmicos reversibles e irreversibles. En los termogramas obtenidos se analizaron las transiciones de primer y segundo orden, en el presente trabajo nos enfocamos en las transiciones de segundo orden, las cuales son asociadas al reordenamiento molecular, principalmente en la temperatura de transición vítrea (Tg). El valor de la Tg para Lβ se estableció en promedio como -12.7±0.43 °C, para las muestras en intervalo de a_w de 0.07 a 0.742, independientemente de la temperatura de almacenamiento. La molécula de Lβ en estado puro presento un solo evento térmico, mientras que para las muestras almacenadas a una a_w superior a 0.742 se observaron dos eventos térmicos, que están relacionados con la presencia de los anómeros Lβ y Lα•H2O. El valor de la Tg para Lα•H2O fue de 80.3, 63.9 y 79.8 °C, para 15, 25 y 35 °C respectivamente.

Los datos obtenidos de las isotermas de sorción y la caracterización fisicoquímica de Lβ, se utilizaron para construir un diagrama de estado, a partir de este se determinó visualmente que la a_w de 0.742 delimita la región de estabilidad entre los anómeros Lβ y Lα•H2O. Para a_w de 0.742 y 0.848 a 15 y 25 °C, se observó una región en donde coexiste los dos anómeros. Con relación a las muestras sometidas a a_w de 0.742 hasta 0.972 y 35 °C, se determinó como la región de Lα•H2O, que se caracteriza como la región en donde las muestras absorbieron una cantidad de agua más allá del contenido de agua en la monocapa. El diagrama de estado corrobora la información obtenida de las diferentes técnicas de caracterización, demostrando la gran estabilidad de Lβ, así como también, contribuye a establecer las condiciones de almacenamiento en cuanto a humedad relativa y temperatura donde se mantiene estable este anómero.

Conclusiones

El estudio de las formas cristalinas de la lactosa se ha realizado desde hace años, sin embargo, en la mayoría de los trabajos realizados el principal impedimento es la obtención de sus anómeros 100% puros. En este trabajo se puso a prueba la estabilidad de Lβ en estado puro a diferentes condiciones de humedad relativa y temperatura. Las muestras de Lβ fueron almacenadas en un intervalo de a_w de 0.07 hasta 0.972, a tres diferentes temperaturas 15, 25 y 35 °C, para su posterior caracterización fisicoquímica. Con ayuda de las técnicas de caracterización fue posible determinar que a valores de a_w superiores a 0.742 se llevó a cabo el proceso de mutarrotación, generando la interconversión de anómero Lβ al anómero Lα•H2O. El diagrama de estado demostró las regiones donde el anómero Lβ se conservaba estable, así como también, la región donde existe la mezcla de ambos anómeros y la región donde solo existe la presencia de Lα•H2O, como resultado del proceso de mutarrotación. Adicionalmente se determino la Tg de Lβ a partir de MDSC, obteniendo un valor Tg=-12.7±0.43 °C. Este estudio contribuye con la generación de información sobre el comportamiento de Lβ puro sometida a diferentes condiciones de almacenamiento y el efecto de la humedad en la interconversión entre los anómeros de lactosa.

Bibliografía

1. Allan, M. C., Grush, E., & Lisa J. Mauer, L. J. (2020). RH-temperature stability diagram of α- and β-anhydrous and monohydrate lactose crystalline forms. Food Research International, 127, 108717. doi.org/10.1016/j.foodres.2019.108717
2. Beebe, J. M., & Gilpin, R. K. (1983). Determination of α-and β-lactose in dairy products by totaly aqueous liquid chromatrography. Analytica Chimica Acta, 146, 255-259. doi.org/10.1016/S0003-2670(00)80613-3
3. Brunauer, S., Deming, LS, Deming, WE y Teller, E. (1940). Sobre una teoría de la adsorción de gases de van der Waals. Revista de la sociedad química estadounidense , 62 (7), 1723-1732. https://doi.org/10.1021/ja01864a025
4. Fox, P. F. (2009). Lactose: Chemistry and properties. In Advanced dairy chemistry (pp. 1-15). Springer, New York, NY.
5. Lara-Mota, E. E., Nicolás–Vázquez, M. I., López-Martínez, L. A., Espinosa-Solis, V., Cruz Alcantar, P., Toxqui-Teran, A., & Saavedra-Leos, M. Z. (2021). Phenomenological study of the synthesis of pure anhydrous β-lactose in alcoholic solution. Food Chemistry, 340, 128054. doi.org/10.1016/j.foodchem.2020.128054
6. Listiohadi, Y. D., Hourigan, J. A., Sleigh, R. W., & Steele, R. J. (2005a). Properties of lactose and its caking behaviour. Australian Journal of Dairy Technology, 60(1), 33.
7. Villafuerte, R. (2011). Los excipientes y su funcionalidad en productos farmacéuticos sólidos The excipients and their functionality in pharmaceutical solid products. Mexican Journal of Pharmaceutical Sciences, 42(1870–0195), 18–36.
8. Walstra, P. y Jenness, R. (1984). Dairy Chemistry and Physics, John Wiley and Sons, New York, pp. 27-41.

Reseña del artículo: Cutting-edge advances on the stability and state diagram of pure β-lactose

El artículo correspondiente a este trabajo fue enviado para su publicación a una revista científica indexada (ANEXO)

ANEXO: MANUSCRITO ENVIADO

Confirm co-authorship of submission to Carbohydrate Polymers

CP

em.carbpol.0.74a26f.7e252968@editorialmanager.com en nombre de
Carbohydrate Polymers <em@editorialmanager.com>
Mié 14/07/2021 12:28
Para: EDGAR ENRIQUE LARA MOTA

This is an automated message.

Journal: Carbohydrate Polymers
Title: Cutting-edge advances on the stability and state diagram of pure β-lactose
Corresponding Author: Dr. María Zenaida Saavedra-Leos
Co-Authors: Edgar Lara- Mota, Agro-industrial Engineer; César Cutberto Leyva Porras, Ph.D; Vicente Espinoza-Solís, Doctor; Claudia Alvares-Salas, Doctor; Alberto Toxqui-Terán, Doctor
Manuscript Number:

Dear Edgar Lara- Mota,

The corresponding author Dr. María Zenaida Saavedra-Leos has listed you as a contributing author of the following submission via Elsevier's online submission system for Carbohydrate Polymers.

Submission Title: Cutting-edge advances on the stability and state diagram of pure β-lactose

Elsevier asks all authors to verify their co-authorship by confirming agreement to publish this article if it is accepted for publication.

Please read the following statement and confirm your agreement by clicking on this link:
https://www.editorialmanager.com/carbpol/l.asp?i=1288160&l=0XF2MAUO

I irrevocably authorize and grant my full consent to the corresponding author of the manuscript to: (1) enter into an exclusive publishing agreement with Elsevier on my behalf (or, if the article is to be published under a CC BY license, a non-exclusive publishing agreement), in the relevant form set out at www.elsevier.com/copyright ; and (2) unless I am a US government employee, to transfer my copyright or grant an exclusive license of rights to Elsevier as part of that publishing agreement, effective on acceptance of the article for publication. If the article is a work made for hire, I am authorized to confirm this on behalf of my employer. I agree that the copyright status selected by the corresponding author for the article if it is accepted for publication shall apply and that this agreement is subject to the governing law of the country in which the journal owner is located.

If you did not co-author this submission, please contact the corresponding author directly at zenaidasaavedra200779@gmail.com.

Thank you,

Carbohydrate Polymers

Carbohydrate Polymers

Cutting-edge advances on the stability and state diagram of pure β-lactose

--Manuscript Draft--

Manuscript Number:	
Article Type:	Research Paper
Keywords:	β-lactose stability; lactose mutarotation; equilibrium state diagram; thermal characterization; technological application
Corresponding Author:	María Zenaida Saavedra-Leos, Ph.D. Autonomous University of San Luis Potosi Matehuala, MEXICO
First Author:	Edgar Lara- Mota, Agro-industrial Engineer
Order of Authors:	Edgar Lara- Mota, Agro-industrial Engineer
	César Cutberto Leyva Porras, Ph.D
	Vicente Espinoza-Solís, Doctor
	Claudia Alvares-Salas, Doctor
	Alberto Toxqui-Terán, Doctor
	María Zenaida Saavedra-Leos, Ph.D.
Abstract:	For this, adsorption isotherms were built at three storage temperatures (15, 25 and 35 ° C) in a wide range of water activity (0.07-0.972). The powders obtained were characterized by Raman spectroscopy, X-ray diffraction (XRD), scanning electron microscopy (SEM), and modulated differential scanning calorimetry (MDSC). The results showed a high stability of Lβ at the storage temperatures, indicating an adsorption similar to the monolayer content. Conversely, the mutarotation process was triggered by the adsorption of water beyond the monolayer content. Under these conditions, the presence of alpha lactose (Lα) was observed. Furthermore, the Tg of the Lβ was determined in the range of -15 to -1.4 °C at the storage conditions. The present work contributes to the study of the stability of Lβ to establish its technological application as a carrier agent or in the microencapsulation of active ingredients.
Suggested Reviewers:	LEIF H SKIBSTED, Doctor 1, Royal Veterinary and Agricultural University: Kobenhavns Universitet Sundhedsvidenskabelige Fakultet is@kvl.dk Lactose stability research
	Hugo Espinosa-Andrews, Doctor 2, Centro de Investigación y Asistencia en Tecnología y Diseño del Estado de Jalisco: Centro de Investigacion y Asistencia en Tecnologia y Diseno del Estado de Jalisco hespinosa@ciatej.mx Works state diagrams of powdered products
	J S Schmidt, Doctor 3, University of Illinois at Urbana-Champaign Department of Food Science and Human Nutrition sjs@illinois.edu Works phase diagrams

Powered by Editorial Manager® and ProduXion Manager® from Aries Systems Corporation

Highlights

- The state diagram of b-lactose is a useful tool to visualize the stability limits to different conditions of temperature and water activity.
- The b-lactose showed a high stability at the storage temperatures.
- Above a water activity of 0.742, the mutarotation process was triggered, producing the appearance of the α-lactose anomer.

Manuscript Click here to view linked References

Cutting-edge advances on the stability and state diagram of pure β-lactose

Edgar Enrique Lara-Mota[1], Cesar Leyva-Porras[2], Vicente Espinosa-Solis[3], Claudia Alvares-Salas[1] Alberto Toxqui-Terán[4], and María Zenaida Saavedra-Leos[5*]

[1] Universidad Autónoma de San Luis Potosí, Facultad de Ingeniería, San Luis Potosí, SLP 78290, México.

[2] Centro de Investigación de Materiales Avanzados S.C (CIMAV), Complejo Industrial Chihuahua. Chihuahua, Chih. 31136. México

[3] Coordinación Académica Región Huasteca Sur, Universidad Autónoma de San Luis Potosí, Km 5, Carr Tamazunchale-San Martin, Tamazunchale, S.L.P. C.P. 79960, México.

[4] Centro de Investigación de Materiales Avanzados S.C. (CIMAV-Mty), Parque de Investigación e Innovación Tecnológica, Apodaca, Nuevo León 66600, México

[5] Coordinación Académica Región Altiplano, Universidad Autónoma de San Luis Potosí, 11 Carretera Cedral Km, 5+600 Ejido San José de las Trojes Matehuala, S.L.P. C.P. 78700, México.

* Corresponding Author. E-mail address: zenaida.saavedra@uaslp.mx

Abstract

A state diagram is a useful tool to visualize the stability limits of a material subjected to different conditions. In this work, the equilibrium state diagram for pure anhydrous beta lactose (Lβ) stability is reported. For this, adsorption isotherms were built at three storage temperatures (15, 25 and 35 ° C) in a wide range of water activity (0.07-0.972). The powders obtained were characterized by Raman spectroscopy, X-ray diffraction (XRD), scanning electron microscopy (SEM), and modulated differential scanning calorimetry (MDSC). The results showed a high stability of Lβ at the storage temperatures, indicating an adsorption similar to the monolayer content. Conversely, the mutarotation process was triggered by the adsorption of water beyond the monolayer content. Under these conditions, the presence of alpha lactose (Lα) was observed. Furthermore, the Tg of the Lβ was determined in the range of -15 to -1.4 °C at the storage conditions. The present work contributes to the study of the

stability of Lβ to establish its technological application as a carrier agent or in the microencapsulation of active ingredients.

Keywords: β-lactose stability; lactose mutarotation; equilibrium state diagram; thermal characterization; technological application.

1. Introduction

Lactose (β-D-galactopyranosyl-D-glucopyranose) is a disaccharide composed of galactose and glucose linked by a β-(1,4) glycosidic bond (Allan, Grush, & Mauer, 2020). As reducing sugar, lactose partially exists as an open chain with a free aldehyde group, which can form a cyclic structure through a hemiacetal bond. With the formation of the hemiacetal bond, a new chiral center is generated, giving rise to isomers or anomers named as α and β (Fox, 2009). These stereoisomers differ in the position of the hydroxyl group of the anomeric carbon in the glucose molecule. In solution, the transformation process between the α and β forms is called mutarotation (Holsinger, 1997). Crystalline lactose is predominantly in the form of α-lactose monohydrate (Lα•H_2O) with a molar ratio lactose to water of 1:1. However, three different anhydrate polymorphic forms are known: anhydrous β-lactose (Lβ), unstable hygroscopic anhydrous α-lactose (LαH), and stable anhydrous α-lactose (LαS) (Kirk, Dann, & Blatchford, 2007). The crystalline form of lactose depends on the processing variables such as drying method (lyophilization, and vacuum dehydration) (Pikal, Lang, & Gaines, 1977; Sebhatu, Angberg, & Ahlneck, 1994), the content of adsorbed water (Fox, 2009), and the temperature exerted during crystallization and storage (Allan et al., 2020). Lopez-Pablos et al. (2018) found a narrow temperature window of 29 and 31 °C for obtaining pure crystalline anhydrous Lβ from a basic alcoholic solution without stirring. Later, Lara-Mota et al. (2021) reported the extension of the temperature interval to 65 °C under reflux conditions, in 2-16 hours and with low concentrations of NaOH and KOH as catalysts.

The technological applications of the different isomers of lactose depend on their physicochemical properties. As an excipient in drugs, α-lactose is used in tablets due to its pleasant taste and high solubility in the digestive tract, protecting the active ingredient from the pH conditions of fluids in the tract and stomach. From the polymorphic forms, the Lβ anomer is the most stable. For example, the use of Lβ in tablets has shown a better

compaction capacity (Lamešić, Planinšek, Lavrič, & Ilić, 2017). Additionally, changes in the particle morphology of the crystallized material affect the physical properties of the final product, such as the fluidity and compaction behavior of the product (Dwivedi & Mitchell, 1989). The stability of lactose employed as excipients in pharmaceutical formulations may depend on the content of the different polymorphs, changes in the crystalline structure, and the collapse of the microstructure (powder agglomeration). These characteristics are closely related to the content of adsorbed humidity and temperature conditions during the storage of the product (Villafuerte, 2011). The change in the stability due to humidity is caused by the plasticizing effect exerted by the water molecules on lactose, affecting the intermolecular interactions and the molecular arrangement of the system (Li, Roos, & Miao, 2015). In this sense, hydrogen bonds are the interactions responsible for maintaining carbohydrates' conformational structure (Lee, Singh, & Kim, 2006). In the adsorption mechanisms, water molecules adhere to lactose molecules by replacing the weakest intramolecular hydrogen bond (Carcabal et al., 2005). As a result, the water adsorption process tends to increase the free volume in the solid. Consequently, the new hydrogen bonds interactions developed favors the molecular mobility, decreasing the glass transition temperature (Tg). In the case of amorphous lactose, the less ordered molecular packing adsorbs large amounts of water, while on the contrary, in the ordered structure of crystalline lactose, water adsorption is substantially lower than in amorphous lactose.

A state diagram is a graphical representation of the properties of a system subjected to different conditions of humidity, composition, temperature, and pressure (Leyva-Porras, López-Pablos, Alvarez-Salas, Pérez-Urizar, & Saavedra-Leos, 2014). State diagrams also provide information about crystallization, glass transition, water solubility, and water freezing. In the food industry, state diagrams are employed to determine the physicochemical properties of simple and complex food systems and predict the stability of dehydrated and frozen products (Sablani, Syamaladevi, & Swanson, 2010; Bhandari & Roos, 2017; Grajales-Lagunes et al., 2018). Several works have focused on developing of state diagrams for pure compounds as model systems for understanding their behavior, and subsequent inclusion in more complex food systems (Bhandari & Roos, 2017). For example, Leyva-Porras et al. (2017) reported the state diagrams for the stability of inulin systems with different degree of polymerization (DP). They found that high DP inulin showed a single state change from

amorphous to crystalline at a water activity (a_w) of 0.5, while the low DP inulin showed an intermediate semicrystalline state at a_w between 0.3-0.5. Furthermore, as the system becomes more complex by the addition of low molecular weight sugars from orange juice, the intermediate semicrystalline interval increases, i.e., from a_w of 0.2-053 (Leyva-Porras et al., 2014). Recently, Allan et al. (2020) reported the relative humidity (RH) diagrams for lactose anomers and hydrate forms in the temperature range of 20-50. They found that the anhydrate to hydrate boundaries increased with the adsorption of RH in that range of temperatures.

Based on these concepts and the physicochemical characterization results. This work reports the state diagrams for the stability of pure β-lactose stored in a temperature range of 15-35 °C and at a_w of 0.07-0.97. We hypothesis that the variation in relative humidity and temperature during storage of crystalline β-lactose affects its chemical and physical stability, inducing interconversion to α-lactose monohydrate anomer. The work also contributes to the thermal characterization of the disaccharide and its technological application as a carrying agent in either the pharmaceutical and food industries.

2. Materials and methods

2.1 Materials.

α-Lactose monohydrate, (L$\alpha \cdot H_2O$, purity ≥ 99.9%) purchased from Sigma-Aldrich Chemical Co., Methanol (MeOH, reagent grade ≥ 99.8) from J.T. Baker, Sodium Hydroxide (KOH, reagent grade ≥ 90%) from Fermont, and distilled water, were employed as reactants for obtaining pure Lβ. The inorganic salts used for subjecting the lactose powders to different conditions of humidity were purchased from Fermont with a purity ≥ 90%: Sodium Hydroxide (NaOH), Potassium Acetate (CH_3COOK), Magnesium Chloride ($MgCl_2$), Potassium Carbonate (K_2CO_3), Magnesium Nitrate [$Mg(NO_3)_2$], Nitrate of Sodium (NaNO3), Potassium Chloride (KCl) and Potassium Sulfate ($K2SO_4$).

2.2 Preparation of β-lactose (Lβ)

Pure anhydrous Lβ was obtained by following the method described by Lara-Mota et al. (2021). In a regular reaction, 15 g of α-lactose monohydrate were mixed in an Erlenmeyer flask with 150 mL of 0.014 M KOH in 95% MeOH. The mixture was refluxed at 65 °C for two hours and filtered after cooled down. The pH of the wet powder was adjusted to 7.25 by

124 washing with a 0.00014 M HNO_3 in 95% MeOH solution. The samples were dried at room
125 temperature overnight.
126
127 *2.3 Determination of water sorption isotherms*
128 Sorption isotherms were constructed by the static gravimetric method (Labuza, Lomauro, &
129 Bakashi, 1985) at temperatures of 15, 25, and 35 °C. The initial moisture content of Lβ was
130 determined by the drying method. The isotherm points were obtained by subjecting the Lβ
131 at different relative humidity conditions in the range a_w of 0.07-0.972. Each
132 microenvironment contained 2 g of Lβ and 100 g of inorganic salt. The systems were
133 equilibrated for 7 days at the desired temperatures. The samples were weighed every 24 h
134 until reaching a constant weight with a difference of ± 0.001 g. Then, the equilibrium
135 moisture content was calculated. Once the sorption isotherms were obtained, a mathematical
136 adjustment was carried out using the model proposed by Guggenheim, Anderson, and Boer
137 (GAB) (Stępień, Witczak, & Witczak, 2020), described by the equation (1).
138 $$Xe = \frac{XmCKa_w}{(1-Ka_w)(1-Ka_w+CKa_w)} \qquad \text{Equation (1)}$$
139 Where: *Xe* is the moisture content at equilibrium (g H_2O/g of dry material), *Xm* is the
140 moisture content of the monolayer (g H_2O/g of dry material), a_w is the water activity, while
141 *K* and *C* are the model constants.
142
143 *2.4 Physicochemical characterization analysis*
144 *2.4.1 Raman spectroscopy*
145 Raman spectroscopy was carried out using a Horiba LabRam HR Evolution instrument with
146 a Jobin Yvon spectrometer and a red laser of He-Ne of 633 nm of wavelength. An Olympus
147 BXFM-ILHS microscope with a 100x objective lens was used to focus the laser beam on the
148 sample. The Raman spectra were collected in a range of 50 to 1500 cm^{-1}.
149
150 *2.4.2 Identification of crystalline phases by X-ray diffraction*
151 Microstructural characterization was determined by X–ray diffraction (XRD) analysis in a
152 D8 Advance ECO diffractometer (Bruker, Karlsruhe, Germany) equipped with Cu-K
153 radiation (l = 1.5406 Å) operated at 45 kV, 40 mA, and an X'Celerator detector in a Bragg-

Brentano geometry. Scans were performed in the 2θ range of 5-50°, with a step size of 0.016° and 20 s per step.

2.4.3 Scanning Electron Microscopy (SEM)

A scanning electron microscope JSM-7401F (JEOL, Japan) operated at 2 kV was employed to observe the morphology of the particles. For reducing the charging effects, each sample was dispersed on a double-side carbon film and covered with a thin layer of gold by sputtering.

2.4.3 Thermal analysis by Modulated Differential Scanning Calorimetry (MDCS)

The glass transition temperature (Tg) was determined using the methodology proposed by Saavedra-Leos et al. (2012). A modulated differential scanning calorimeter (MDSC) model Q200, (TA Instruments, Lukens Drive, New Castle, DE), equipped with an RCS90 cooling system was used. The instrument was calibrated for temperature and enthalpy using indium as standard, while sapphire was used for heat capacity. HPLC grade nitrogen with a flow rate of 100 mL/min was used as purge gas to generate an inert atmosphere. A powder sample of 10 mg was weighed into sealed Tzero^{TM} aluminum cells. The thermal program heating and cooling ramps were carried out with a modulation of 40 s, and amplitude of 1.5 °C. Thermograms were acquired by following the next procedure: (i) isothermal at -50 °C for 1 minute, (ii) heating from -50 to 190 °C at 20 °C/min, (iii) isothermal at 190 ° C for 1 minute, (iv) cooling from 190 to -50 °C at 10 °C/min, (v) heating from -50 to 300 °C at 10 °C/min. The thermograms obtained were analyzed using Universal Analysis 2000 software, version 4.4A, to determine the glass transition of cooling (T_{gC}) and the glass transition of heating (T_{gH}).

3. Results and Discussion

3.1 Sorption isotherms

The Lβ isotherms at 15, 25, and 35 °C are presented in Fig 1. Despite the temperature, the isotherms presented a constant water content in the water activity range of 0.07-0.742. The adsorbed water content was 0.07 g H_2O/g of dry material. For a_w greater than 0.742, an asymptotic behavior was observed, indicating the increase of water adsorption. At these

185 humidity conditions, the temperature clearly affected the water content as 0.55, 1.25, and
186 2.58 g H_2O/g of dry material, for 15, 25, and 35 °C, respectively. These results agree with
187 those reported by Bronlund & Paterson (2004), who indicated that at a_w of 0.85, amorphous
188 and crystalline α-lactose adsorbed 10% and 0.7% g of H_2O/g of dry material, respectively,
189 followed by an exponential increase. For spray-dried lactose and α-lactose monohydrate, the
190 water content was 0.25 and 0.1 g of H_2O/g of dry material, at a_w of 0.45 and 0.75, respectively
191 (Shrestha, Howes, Adhikari, & Bhandari, 2007).
192 Brunauer, Deming, Deming, & Teller (1940) described five types of isotherms for porous
193 materials. The shape of the Lβ isotherms corresponded to the isotherm type III, which is
194 characteristic of materials rich in soluble substances of low molecular weight, such as organic
195 acids and sugars (Stępień et al., 2020). Table 1 presents the fitted parameters of the GAB
196 model. The moisture content of the monolayer (Xm) indicates the amount of water interacting
197 directly with the solute, forming a single layer of water molecules adsorbed on the surface of
198 the solid. This parameter is related to the storage conditions and stability of the food product
199 (Sormoli & Langrish, 2014). Although the three systems showed relatively low monolayer
200 water content, i.e., $0.02<Xm<0.04$, the shape of the isotherm is linear in the region of a_w of
201 0.07-0.742. This observation suggested that the adsorption of water is close to the monolayer
202 content in this region of the isotherm. The concept of the content of the monolayer is related
203 to the stability of the product, in the sense that as the moisture adsorption remains below this
204 value, the physicochemical and microstructural properties will remain unchanged. The
205 energy constant (C) determines the binding force of water molecules to the primary binding
206 sites on the surface of the solid. The calculated values for the three temperatures were similar,
207 indicating a high interaction energy between the solid and the solvent, and the independence
208 of this energy with the temperature. The parameter K describes the multilayer interactions
209 between water molecules and the solid (Quirijns, Van Boxtel, Van Loon, & Van Straten,
210 2005). These calculated values showed a slight decrease with the temperature. Based on these
211 results, the Lβ may present high stability when stored at the conditions of water activity in
212 the range of 0.07-0.742 and temperatures of 15-35 °C.
213
214 *3.2 Chemical analysis*

With Raman spectroscopy is possible to distinguish differences in microstructure, composition, and how the atoms are linked to each other (Smith & Clark, 2004). Lactose molecule presents vibrational modes in the wavenumber range of 100-1200 cm^{-1}. The vibration mode at 357 cm^{-1} is attributed to the torsional of the COOH and HOH groups. The vibration modes at 477 and 633 cm^{-1} are attributed to the deformation of the CCO group in the glycosidic bond. The vibration modes at 953 and 1142 cm^{-1} are generated by the stretching of the CO bond in the glycosidic bond (López-Pablos et al., 2018; Wiercigroch et al., 2017). Fig. 2 shows the Raman spectra for Lβ in the a_w range of 0.07-0.972, at temperatures of 15, 25, and 35 °C. The vibrations characteristic for β-lactose are observed at 357 cm^{-1} as a double peak, and a double low-intensity vibration at 1100 cm^{-1} (López-Pablos et al., 2018). In contrast, Lα monohydrate presents single high-intensity vibration modes at wavenumbers of 357 and 1086 cm^{-1} (Wiercigroch et al., 2017; Islam & Langrish, 2010; Kirk et al., 2007; Murphy, Prescott, & Larson, 2005). With these vibrations modes, it was possible to identify the mutarotation process of Lβ into Lα at the different storage conditions. The systems at 15, 25 and 35 °C behaved in a similar way. The Lβ remained stable with the adsorption of water up to a water activity of 0.742, while above the Lα was observed.

3.3 Microstructural identification

Fig. 3 shows the X-ray diffractograms for Lβ in the a_w range of 0.07-0.972, at temperatures of 15, 25, and 35 °C. The diffraction patterns were compared with the powder diffraction file (PDF) reported by the International Center for Diffraction Data (ICDD), PDF No. 000291758 and PDF No. 000241783, for Lβ and Lα, respectively. At the lowest a_w (0.07), the diffractograms showed only the diffraction peaks of Lβ, identified at 2θ angles of 10.5, 19, and 21°. This observation remained the same until at a_w of 0.742. After this water activity for storage temperatures of 15 and 25 °C, the mutarotation process was observed as the presence of both anomers, by the characteristic reflections of the Lα anomer at 2θ angles of 12.5, 16.4, 19.5, and 20.5°. However, at the storage temperature of 35 °C, only the Lα anomer was observed. Clearly, the adsorption of water promoted the mutarotation process at higher water content, and this process was accelerated by the increase in the storage temperature.

In addition to the identification of the anomers, the diffraction patterns were useful to know the microstructural state of the powders, i.e., if they are amorphous or crystalline, and to

observe any state change triggered by the adsorption of water. According to Saavedra-Leos, Leyva-Porras, Araujo-Díaz, Toxqui-Terán, & Borrás-Enríquez (2015), in maltodextrins, the amorphous state is observed as a broad peak and the absence of well-defined diffraction peaks, while in inulin, the state change is observed as the development of diffraction peaks with the a_w. The diffractograms reported herein showed well-defined peaks over a linear baseline, indicating the obtaining of anhydrous crystalline Lβ after the synthesis process. Likewise, the conservation of crystalline lactose either β or α, was observed at all the storage conditions of water adsorption and temperature. From the microstructural analysis by XRD, it was possible to confirm the stability of the Lβ subjected to different storage conditions of humidity and temperature.

3.4 Morphological analysis

Fig. 4 shows selected micrographs of the Lβ stored at the initial, intermediate, and extreme conditions of water activity (0.07, 0.538, 0.848, and 0.972) for the three storage temperatures. According to Wong & Hartel, (2014) the crystallization mechanism of α-lactose involves three stages: nucleation, growth, and crystal maturation. Furthermore, the crystallization rate affects the particle morphology (Herrington, 1934). Several authors have reported the particle morphology of Lβ as a curved needle-like prism or an axel-type (Lara-Mota et al., 2021; Lopez-Pablos et al., 2018; Wong, Jenness, Keeney, & Marth, 1999). On the other hand, Lα has been observed as irregular shape particles (Raghavan, Ristic, Sheen, & Sherwood, 2000). In this sense, on the micrographs, the individual particle morphology was identified by the ellipses, in red for Lβ and in yellow for Lα, respectively. As observed, at the initial and intermediate a_w, the micrographs only showed curved-shape particles, corresponding to the Lβ morphology. While at the extreme a_w conditions, a mixture of curved and irregular shape particles was observed, suggesting the presence of both anomers. Evidently, the water adsorption process causes the mutarotation of Lβ into Lα. However, this phenomenon involves not only a change in the position of the functional group of the anomeric carbon in the glucose molecule but also a change in the morphology of the particle.

3.5 Thermal analysis by Modulated Differential Scanning Calorimetry

In modulated differential scanning calorimetry (MDSC), besides the linear heating rate, sinusoidal heating is performed for simultaneously measuring the heat capacity of the sample

and differentiating between the reversible and irreversible thermal events (Leyva-Porras et al., 2019). The reversible heat flux is related to the second-order transitions associated with molecular rearrangements, such as the glass transition temperature. This thermal event is observed as a slight variation in the slope of the heat flow curve. Meanwhile, in the non-reversible heat flow curve, thermal events are related to first-order transitions, characterized by the absorption or release of latent heat, measured through the variation of the enthalpy ΔH, and observed as a phase change, i.e., from solid into a viscous liquid. Fig. 5 shows the selected MDSC thermograms for the Lβ powders subjected to the different conditions of water activity and temperature. The thermograms show the total heat flow (sinusoidal curve) and the derivative of the reversible heat flow (regular curve). On the latter, the determined Tg value was indicated with an arrow. Although the MDSC experiments were carried out through several cooling-heating cycles, the Tg was determined from the last heating cycle. Table 2 summarizes the Tg results of the systems subjected to the different storage conditions. Because the glass transition is not presented as a well-defined temperature but involves a range of temperatures, Table 2 reports the initial, middle, and end temperatures where Tg was determined. From these data, the middle temperature was selected as the Tg value. The Tg value of anhydrous Lβ was -12.67±0.43 °C. With the adsorption of water, some Tg values were scattered, but the majority presented similar values, showing a slight increase of 1-2 °C. Contrary to this, other carbohydrate polymers such as maltodextrins and inulin have shown a strong dependence of the Tg with the adsorption of water (Saavedra-Leos et al., 2015; Leyva-Porras et al., 2017). For maltodextrins, Tg drops from 90 to 20 ° C in the a_w range of 0.07-0.75, while for inulin, the Tg decreases from 100 to -40 ° C, in the a_w range of 0.05-0.9. On the other hand, the Tg value slightly decreased with the storage temperature. For example, the average Tg values for storage temperatures of 15, 25, and 35 ° C were -7.5, -8.8, and -11.9 °C, respectively. Clearly, these observations suggested the high thermal stability of Lβ in the range of water activities and storage temperatures tested.

In addition, MDSC was also helpful for identifying the mutarotation of Lβ. Thermograms of samples stored at a_w of 0.07-0.742 showed a single thermal event corresponding to the Tg of pure Lβ. However, the thermograms of samples stored at a_w of 0.972 presented two thermal events, corresponding to the presence of both anomers, Lβ and Lα. The Tg values of the Lα anomer were 80.3, 63.9, and 79.8 °C, for storage temperatures of 15, 25, and 35 °C,

309 respectively. Some works have reported the Tg of α-lactose with the different contents of
310 water. For example, at a_w of 0.23, the Tg of amorphous α-lactose was 43.7 °C (Roos & Karel.
311 1990), while for α-lactose monohydrate, the Tg value was 105 °C (Fan & Roos, 2017).
312
313 *3.6 Equilibrium state diagram of Lβ*
314 Based on the physicochemical characterization of the Lβ powders subjected to different
315 conditions of humidity and temperature, a state diagram was constructed. The regions of the
316 diagram were drawn from the data of the equilibrium isotherms, the thermal, chemical, and
317 microstructural characterization, and the particle morphology analysis. Fig. 6 shows the
318 equilibrium state diagram of Lβ (continuous line) in the water activity range of 0.07-0.972 at
319 storage temperatures of 15, 25, and 35 °C. The top of the Lβ region is defined by the
320 monolayer water content at 0.07 g of water/g of dry material. The water activity of 0.742
321 divides the Lβ region from the Lα. Between the water activities of 0.742-0.848 and the
322 storage temperatures of 15 and 25 °C, there is an intermediate region containing a mixture of
323 both anomers Lβ and Lα. In this region, the water content increases from 0.11 to 0.36 g of
324 water/g of dry material. The Lα region is promoted by the adsorption of water beyond the
325 monolayer content and is inversely influenced by the storage temperature. The Lα region
326 extends from the water activity of 0.742 at the storage temperature of 35 °C until the full
327 saturation of water. This state diagram clearly shows the high stability of the Lβ and sets the
328 storage conditions of water content and temperature.
329 On the top of the diagram, the polygon (dashed line) encloses the determined Tg values of
330 Lβ at the different water activities and storage temperatures. The Tg is included in the state
331 diagram because it is related to the stability of food and pharmaceutical products. When the
332 food product is stored at a temperature above the Tg, the thermal energy provokes the state
333 conversion, and consequently, the change of the physicochemical properties. The Tg values
334 for the Lβ varied in the range of -15 to -1.4 °C. However, even when the Lβ powders were
335 stored at temperatures above the Tg, the mutarotation process was hindered because of the
336 relatively low adsorption of water. Therefore, the stability of the Lβ will conserve as long as
337 the powder be stored at low water content, specifically below the monolayer content.
338 Likewise, the set of storage temperatures (15, 25, and 35 °C) was selected in order to test the
339 stability above and below the room temperature.

4. Conclusions

In this work, the stability of pure anhydrous Lβ powder was tested at different storage conditions of temperature and humidity. Samples were subjected to water activity (a_w) in the range of 0.07-0.972, and the physicochemical properties were characterized. Although the monolayer content determined from the isotherms was relatively low, the Lβ powders adsorbed a water content similar to that value. Above a water activity of 0.742, the mutarotation process was triggered, producing the appearance of the Lα anomer. The physicochemical characterization confirmed the stability of the Lβ, and the presence of the Lα anomer at the higher a_w. An equilibrium state diagram was constructed, showing the region where the Lβ was stable, an intermediate region with a mixture of both anomers, and the region of the Lα obtained from the mutarotation process. The Tg for the Lβ determined from the MDSC experiments showed values in the range of -15 to -1.4 °C. The study was helpful to understand that the Lβ adsorbs low quantities of water in the temperature range of 15-35 °C and that the higher adsorption of water is promoted by the presence of the Lα anomer.

Acknowledgments: The technical support provided by Ernesto Guerrero Lasterjet, and Pedro Pizzá, by the microstructural and chemical characterizations, respectively. In addition, we thank the Laboratorio Nacional de Nanotecnología (Nanotech) for the use of the high-resolution scanning electron microscope.

References:

Allan, M. C., Grush, E., & Lisa J. Mauer, L. J. (2020). RH-temperature stability diagram of α- and β-anhydrous and monohydrate lactose crystalline forms. *Food Research International*, 127, 108717. https://doi.org/10.1016/j.foodres.2019.108717

Bhandari, B. & Roos, Y. (2017) Introduction to Non-Equilibrium States and Glass Transitions—The Fundamentals Applied to Foods Systems. Woodhead Publishing Series in Food Science, Technology and Nutrition. https://doi.org/10.1016/B978-0-08-100309-1.00001-8

Bronlund, J., & Paterson, T. (2004). Moisture sorption isotherms for crystalline , amorphous and predominantly crystalline lactose powders. *International Dairy Journal*, *14*, 247–254. https://doi.org/10.1016/S0958-6946(03)00176-6

Brunauer, S., Deming, L. S., Deming, W. E., & Teller, E. (1940). Theory of the van der waals adsorption of gases. *Journal of the American Chemical Society*, *1139*(6), 1723–1732. https://doi.org/10.1021/ja01864a025

Carcabal, P., Jockusch, R. A., Hu, I., Snoek, L. C., Kroemer, R. T., Davis, B. G., Gamblin, D. P., Compagnon, I., Oomens, J., & Simons, J. P. (2005). Hydrogen Bonding and Cooperativity in Isolated and Hydrated Sugars : Mannose , Galactose , Glucose , and Lactose ¸ arc. *Journal of the American Chemical Society*, *127*, 11414–11425. https://doi.org/10.1021/ja0518575

Dwivedi, S. K., & Mitchell, A. G. (1989). Gas Chromatographic Analysis of Anomeric Composition. *Journal of Pharmaceutical Science*, *78*(12), 1055–1056. https://doi.org/10.1002/jps.2600781217

Fan, F., & Roos, Y. H. (2017). Glass Transition-Associated Structural Relaxations and Applications of Relaxation Times in Amorphous Food Solids: a Review. *Food Engineering Reviews*, *9*(4), 257–270. https://doi.org/10.1007/s12393-017-9166-6

Fox P. (2009) Lactose: Chemistry and Properties. In: McSweeney P., Fox P. (eds) Advanced Dairy Chemistry. Springer, New York, NY. https://doi.org/10.1007/978-0-387-84865-5_1

Grajales-Lagunes, A., Rivera-Bautista, C., Loredo-García, I. O., González-García, R., González-Chávez, M. M., Schmidt, S.J., Ruiz-Cabrera, M. A. (2018). Using model food systems to develop mathematical models for construction of state diagrams of fruit products, *Journal of Food Engineering*, 230, 72-81. https://doi.org/10.1016/j.jfoodeng.2018.02.025

Herrington, B. L. (1934). Some physico-chemical properties of lactose. *Journal of Dairy Science*, *17*, 533–542. https://doi.org/10.3168/jds.S0022-0302(34)93270-7

Holsinger V.H. (1997) Physical and Chemical Properties of Lactose. In: Fox P.F. (eds) Advanced Dairy Chemistry Volume 3. Springer, Boston, MA. https://doi.org/10.1007/978-1-4757-4409-5_1

Islam, M. I. U., & Langrish, T. A. G. (2010). An investigation into lactose crystallization under high temperature conditions during spray drying. *Food Research International*, *43*(1), 46–56. https://doi.org/10.1016/j.foodres.2009.08.010

Kirk, J. H., Dann, S. E., & Blatchford, C. G. (2007). Lactose: A definitive guide to poly-morph determination. *International Journal of Pharmaceutics*, 334(1–2), 103–114. https://doi.org/10.1016/j.ijpharm.2006.10.026

Labuza, T., Lomauro, C., & Bakashi, A. (1985). Moisture Transfer Properties of Dry and Semimoist Foods. *Journal of Food Science*, *50*, 397–400. https://doi.org/10.1111/j.1365-2621.1985.tb13411.x

Lamešić, D., Planinšek, O., Lavrič, Z., & Ilić, I. (2017). Spherical agglomerates of lactose with enhanced mechanical properties. *International Journal of Pharmaceutics*, 5*16 (1-2)*, 247–257. https://doi.org/10.1016/j.ijpharm.2016.11.040

Lara-Mota, E. E., Nicolás–Vázquez, M. I., López-Martínez, L. A., Espinosa-Solis, V., Cruz-Alcantar, P., Toxqui-Teran, A., & Saavedra-Leos, M. Z. (2021). Phenomenological study of the synthesis of pure anhydrous β-lactose in alcoholic solution. *Food Chemistry*, *340*, 128054. https://doi.org/10.1016/j.foodchem.2020.128054

Lee H.M., Singh N.J., Kim K.S. (2006). Weak to Strong Hydrogen Bonds. In: Grabowski S.J. (eds) Hydrogen Bonding—New Insights. Springer, Dordrecht. https://doi.org/10.1007/978-1-4020-4853-1_4

Leyva-Porras, C., Cruz-Alcantar, P., Espinosa-Solís, V., Martínez-Guerra, E., Piñón-Balderrama, C. I., Compean Martínez, I., & Saavedra-Leos, M. Z. (2019). Application of Differential Scanning Calorimetry (DSC) and Modulated Differential Scanning Calorimetry (MDSC) in Food and Drug Industries. Polymers, 12(1), 5. http://dx.doi.org/10.3390/polym12010005

Leyva-Porras, C., López-Pablos, A. L., Alvarez-Salas, C., Pérez-Urizar, J., & Saavedra-Leos, Z. (2014). Physical properties of inulin and technological applications. In: *Ramawat, KG, Mérillon, JM, Eds. Polysaccharides; Springer: New York, NY, USA*, 959-984. https://doi.org/10.1007/978-3-319-03751-6_80-1

Leyva- Porras, C., Saavedra–Leos, M. Z., López- Pablos, A. L., Soto- Guerrero, J. J., Toxqui- Terán, A., & Fozado- Quiroz, R. E. (2017). Chemical, thermal and physical characterization of inulin for its technological application based on the degree of polymerization. *Journal of Food Process Engineering*, 40(1), e12333. https://doi.org/10.1111/jfpe.12333

Li, R., Roos, Y. H., & Miao, S. (2015). The effect of water plasticization and lactose content on flow properties of dairy model solids. *Journal of Food Engineering*, *170*, 50–57. https://doi.org/10.1016/j.jfoodeng.2015.09.014

López-Pablos, A. L., Leyva-Porras, C. C., Silva-Cázares, M. B., Longoria-Rodríguez, F. E., Pérez-García, S. A., Vértiz-Hernández, Á. A., & Saavedra-Leos, M. Z. (2018). Preparation and Characterization of High Purity Anhydrous β -Lactose from α -Lactose Monohydrate at Mild Temperature. *International Journal of Polymer Science*, *2018*. https://doi.org/10.1155/2018/5069063

Murphy, B. M., Prescott, S. W., & Larson, I. (2005). Measurement of lactose crystallinity using Raman spectroscopy. *Journal of Pharmaceutical and Biomedical Analysis*, *38*(1), 186–190. https://doi.org/10.1016/j.jpba.2004.12.013

Pikal, M. J., Lang, J. E., & Gaines, K. (1977). Quantitative Crystallinity Determinations for P-Lactam Antibiotics by Solution Calorimetry : Correlations with Stability. *Journal of Pharmaceutical Science*, *67*(6), 767–773.

Quirijns, E. J., Van Boxtel, A. J. B., Van Loon, W. K. P., & Van Straten, G. (2005). Sorption isotherms , GAB parameters and isosteric heat of sorption. *Journal of the Science of Food and Agriculture*, *1814*, 1805–1814. https://doi.org/10.1002/jsfa.2140

Raghavan, S. L., Ristic, R. I., Sheen, D. B., & Sherwood, J. N. (2000). Morphology of Crystals of r -Lactose Hydrate Grown from Aqueous Solution. *The Journal of Physical Chemistry B*, *104*, 12256–12262. https://doi.org/10.1021/jp002051o

Roos, Y., & Karel, M. (1990). Differential Scanning Calorimetry Study of Phase Transitions Affecting the Quality of Dehydrated Materials. *Biotechnology Progress*, *6*(2), 159–163. https://doi.org/10.1021/bp00002a011

Saavedra-Leos, Maria Zenaida, Alvarez-Salas, C., Esneider, M., Toxqui-Teran, A., Pérez, S., & Ruiz, M. (2012). Towards an improved calorimetric methodology for glass transition temperature determination in amorphous sugars/Metodología calorimétrica mejorada para la determinación de temperaturas de transición vítrea en azúcares amorfos. *CyTA - Journal of Food*, *10*(4), 258–267. https://doi.org/10.1080/19476337.2011.639960

Saavedra-Leos, Z., Leyva-Porras, C., Araujo-Díaz, S., Toxqui-Terán, A., & Borrás-Enríquez, A. (2015). Technological application of maltodextrins according to the degree of polymerization. *Molecules*, 20 (12), 21067–21081. http://dx.doi.org/10.3390/molecules201219746

Sablani, S. S., Syamaladevi, R. M., & Swanson, B. G. (2010). A review of methods, data and applications of state diagrams of food systems. *Food Engineering Reviews*, 2(3), 168–203. https://doi.org/10.1007/s12393-010-9020-6

Sebhatu, T., Angberg, M., & Ahlneck, C. (1994). Assessment of the degree of disorder in crystalline solids by isothermal microcalorimetry. *International Journal of Pharmaceutics*, *104*, 135–144. https://doi.org/10.1016/0378-5173(94)90188-0

Shrestha, A. K., Howes, T., Adhikari, B. P., & Bhandari, B. R. (2007). Water sorption and glass transition properties of spray dried lactose hydrolysed skim milk powder. *LWT - Food Science and Technology*, *40*(9), 1593–1600. https://doi.org/10.1016/j.lwt.2006.11.003

Smith, G. D., & Clark, R. J. H. (2004). Raman microscopy in archaeological science. *Journal of Archaeological Science*, *31*(8), 1137–1160. https://doi.org/10.1016/j.jas.2004.02.008

Sormoli, M. E., & Langrish, T. A. G. (2014). Moisture sorption isotherms and net isosteric heat of sorption for spray-dried pure orange juice powder. *LWT - Food Science and Technology*, 1–8. https://doi.org/10.1016/j.lwt.2014.09.064

Stępień, A., Witczak, M., & Witczak, T. (2020). Sorption properties, glass transition and state diagrams for pumpkin powders containing maltodextrins. *Lwt*, *134*(September). https://doi.org/10.1016/j.lwt.2020.110192

Villafuerte, R. (2011). Los excipientes y su funcionalidad en productos farmacéuticos sólidos The excipients and their functionality in pharmaceutical solid products. *Mexican Journal of Pharmaceutical Sciences*, *42*(1870–0195), 18–36.

Wiercigroch, E., Szafraniec, E., Czamara, K., Pacia, M. Z., Majzner, K., Kochan, K., Kaczor, A., Baranska, M., & Malek, K. (2017). Raman and infrared spectroscopy of carbohydrates: A review. *Spectrochimica Acta - Part A: Molecular and Biomolecular Spectroscopy*, *185*, 317–335. https://doi.org/10.1016/j.saa.2017.05.045

Wong, N. P., Jenness, R., Keeney, M., & Marth, E. H. (1999). Fundamentals o f dairy chemistry, third edition, Aspen publishers, Gaithersburg, Maryland, USA.

Wong, S. Y., & Hartel, R. W. (2014). Crystallization in Lactose Refining — A Review. *Journal of Food Science*, *79*(3), 257–272. https://doi.org/10.1111/1750-3841.12349

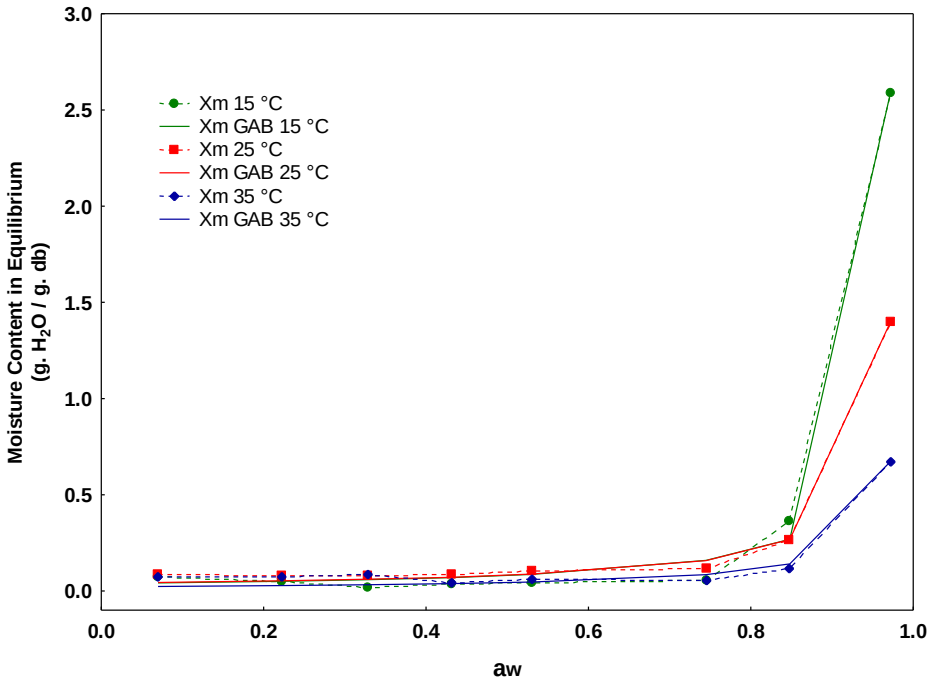


Fig. 1 Water adsorption isotherms at temperatures of 15, 25, and 35 ° C. Dashed lines represent the fitted data by the GAB model.

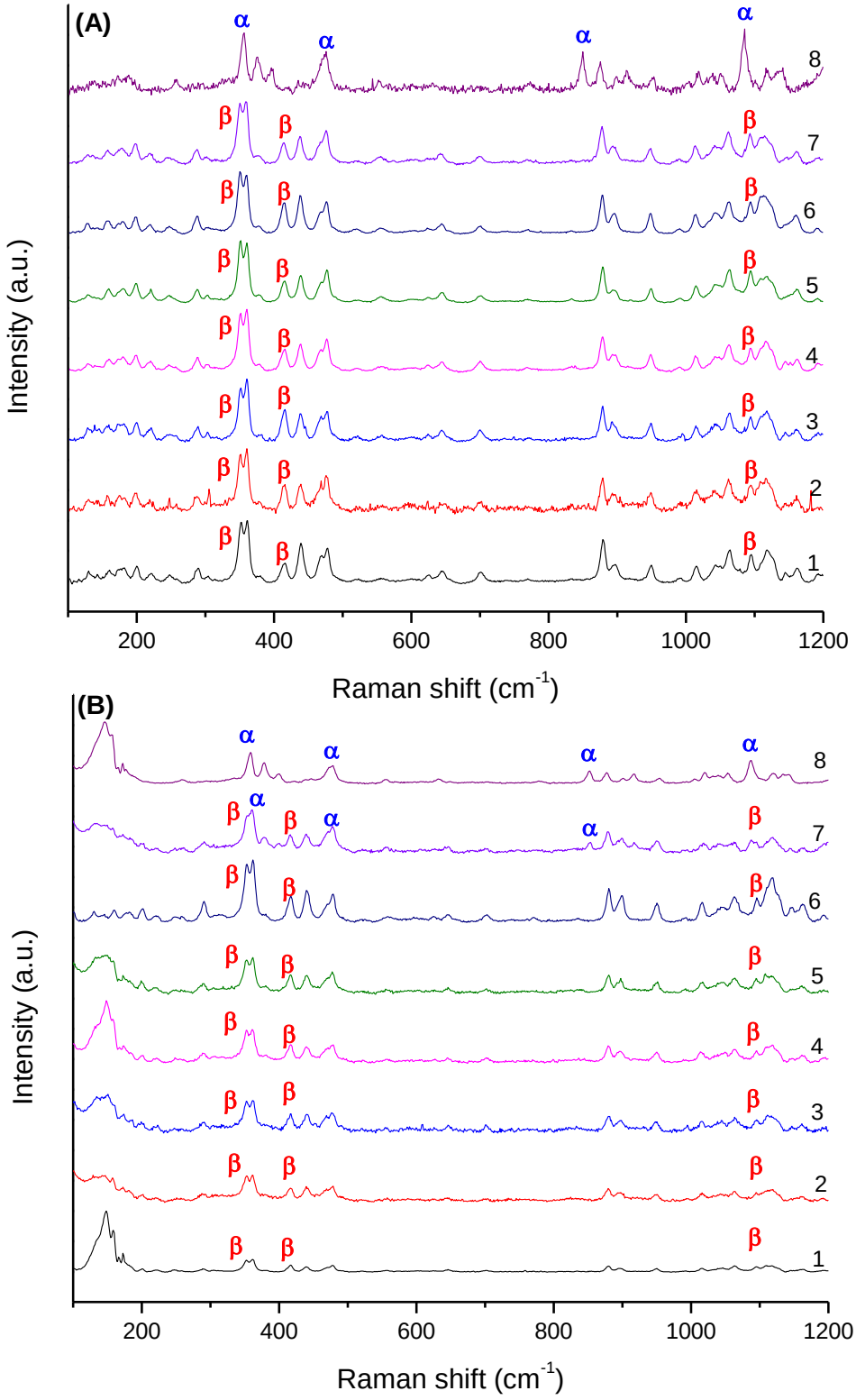


Fig. 2. Raman spectra of β-lactose in the a_w range of 0.07-0.972. (A) 15 °C, (B) 25 °C, and (C) 35 °C. The anomers are identified on each spectrum as α and β.

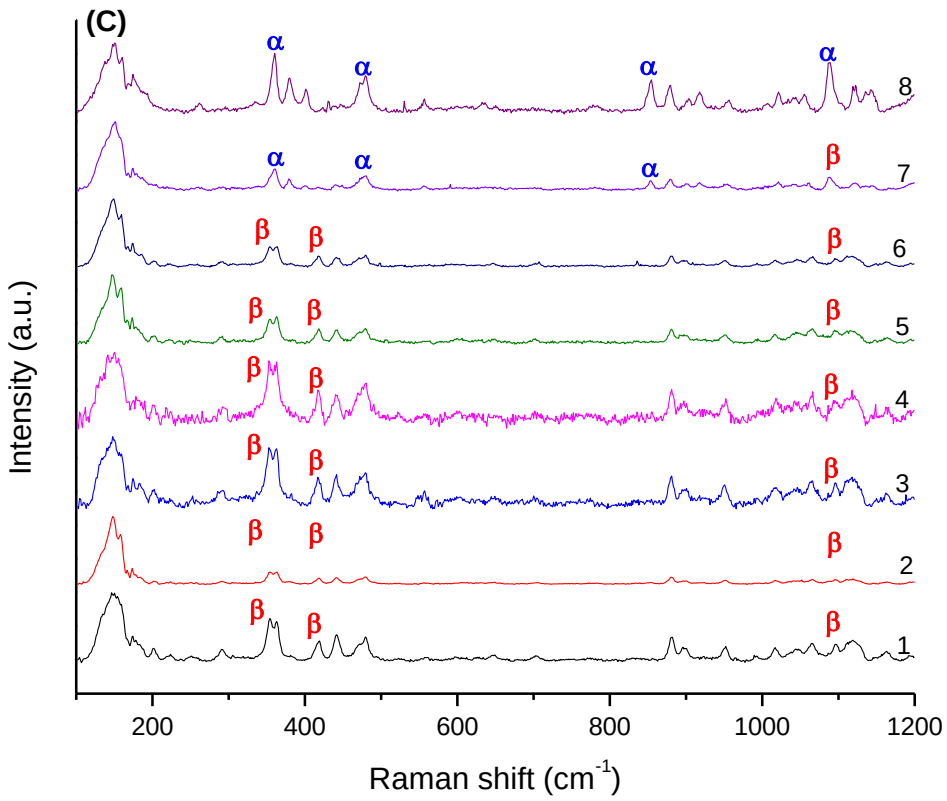


Fig. 2, *continuation*.

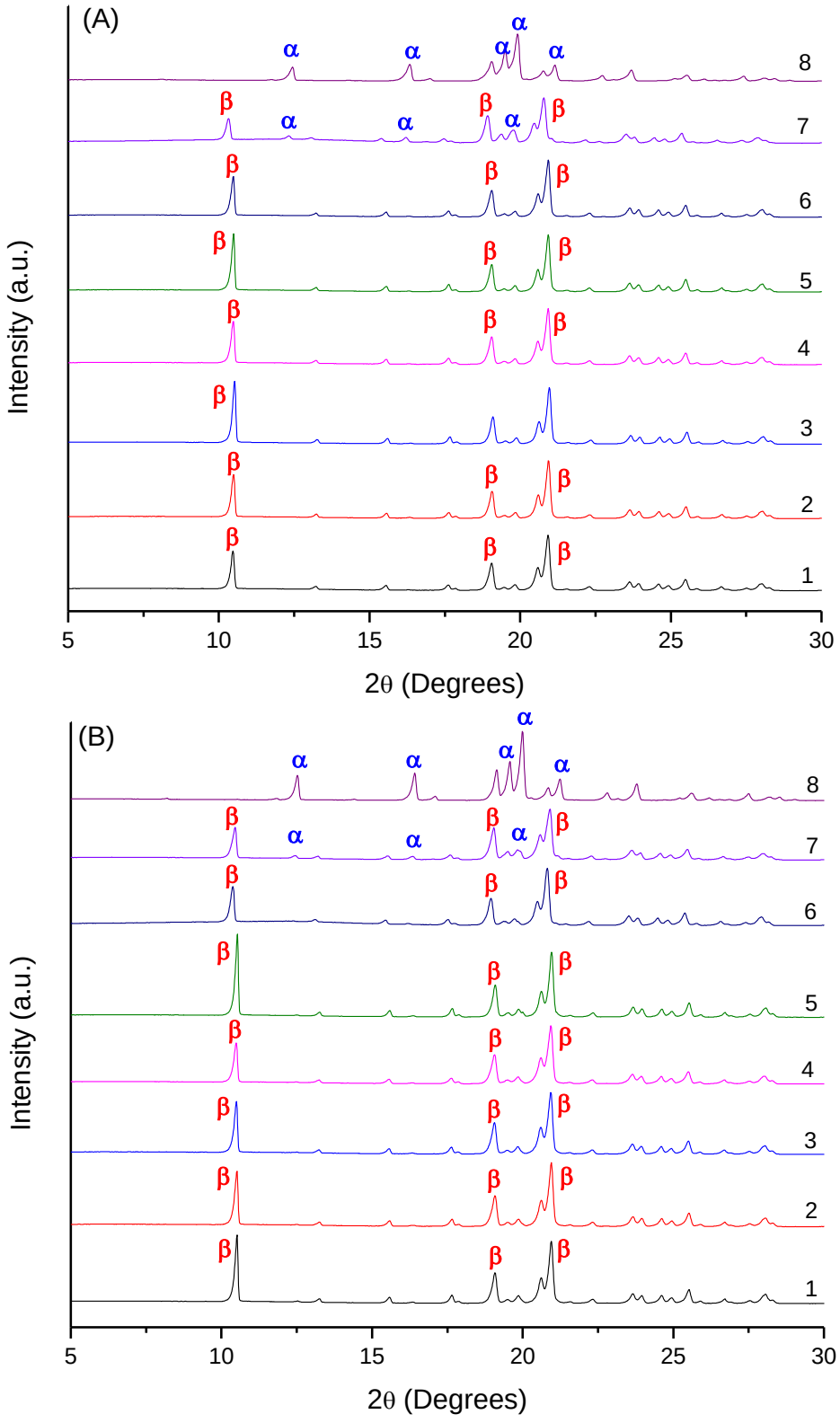


Fig. 3. X-ray diffraction patterns for the stability of Lβ in the water activity range of 0.07-0.972. Adsorption temperature of (A) 15 °C, (B) 25 °C, and (C) 35 °C. The anomers are identified on each diffractogram as α and β.

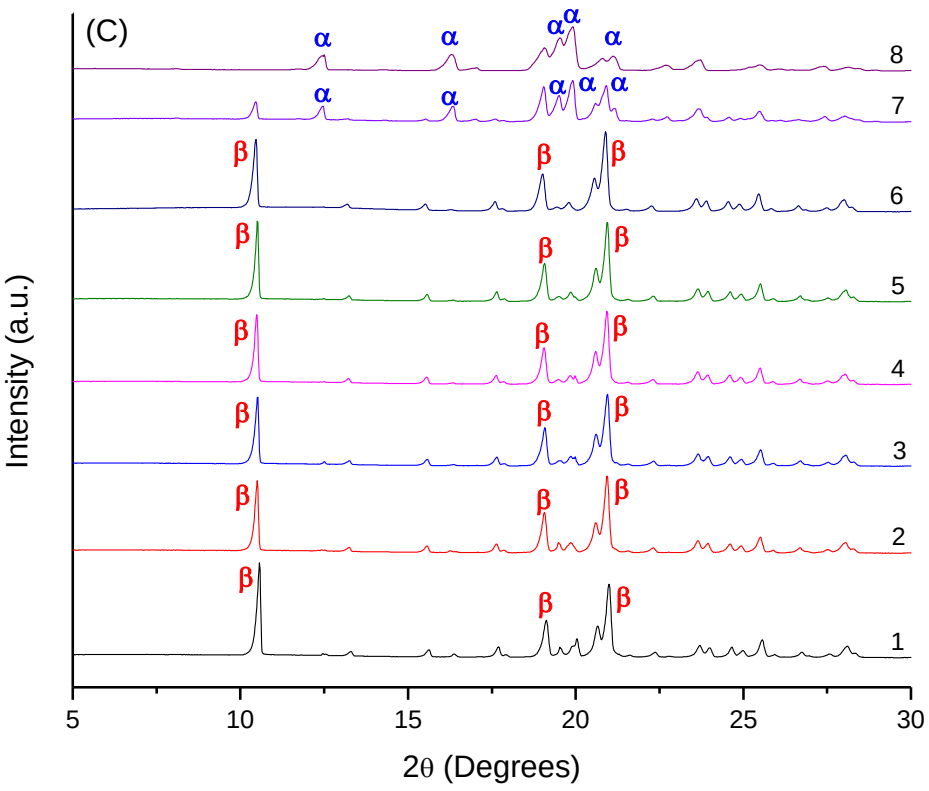


Fig. 3, *continuation*.

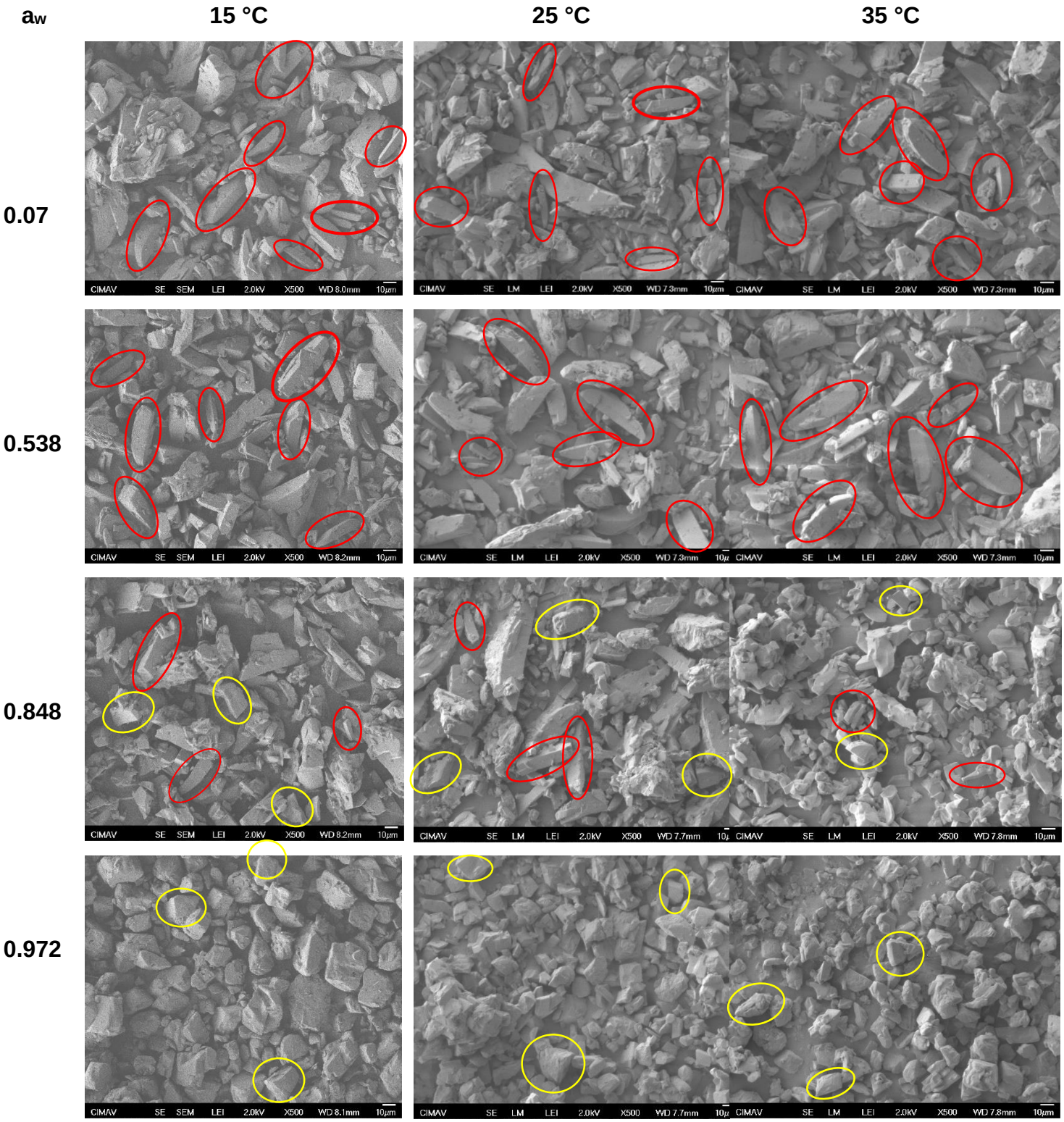


Fig. 4. SEM images for Lβ at selected water activities and storage temperatures of 15, 25, and 35 °C. Lβ and Lα particles are indicated by the red and yellow circles, respectively.

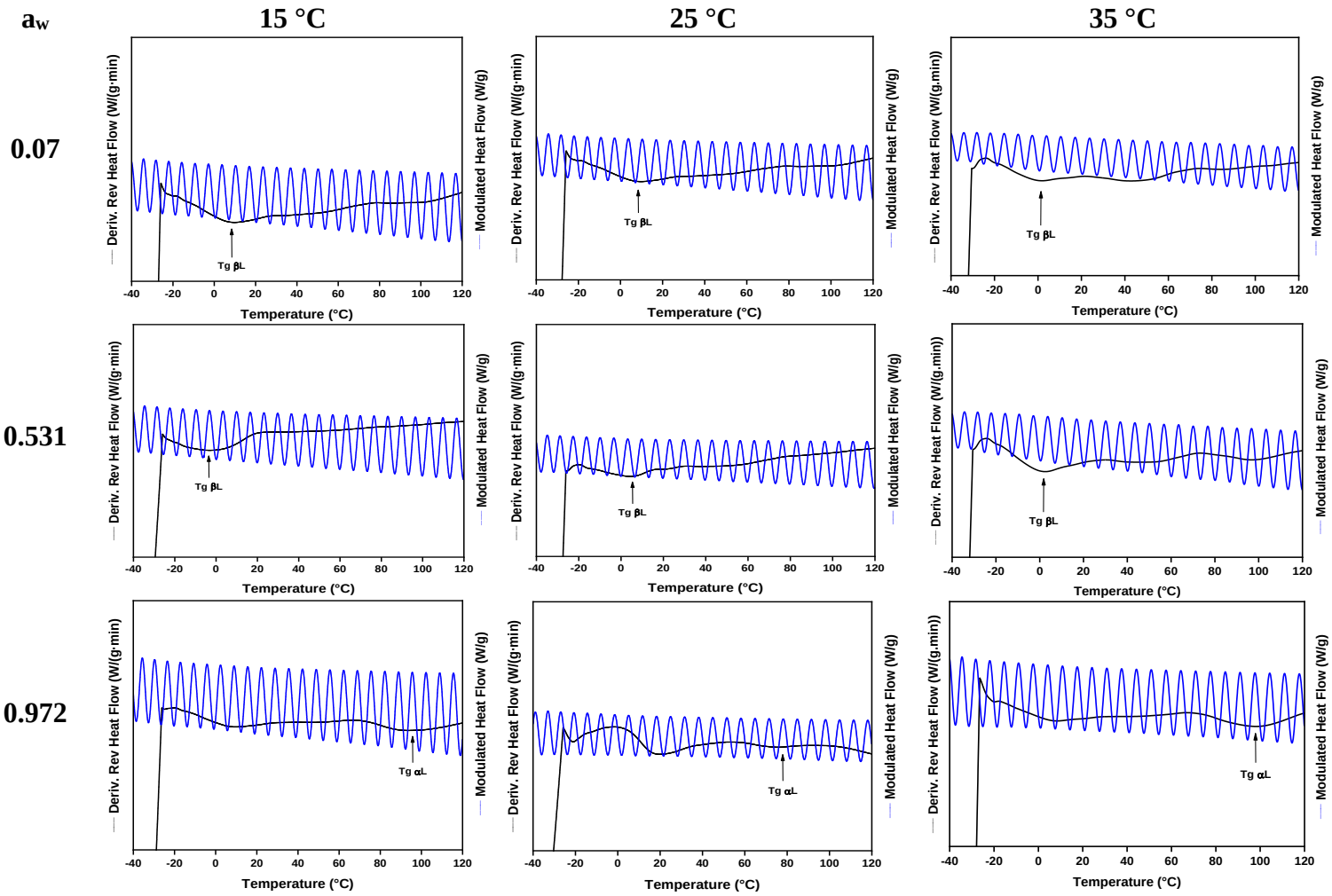


Fig. 5. MDSC thermograms of Lβ at selected water activities and storage temperatures of 15, 25, and 35 °C. Determined Tg value is indicated by the arrow on the derivative of the non-reversible heat flow.

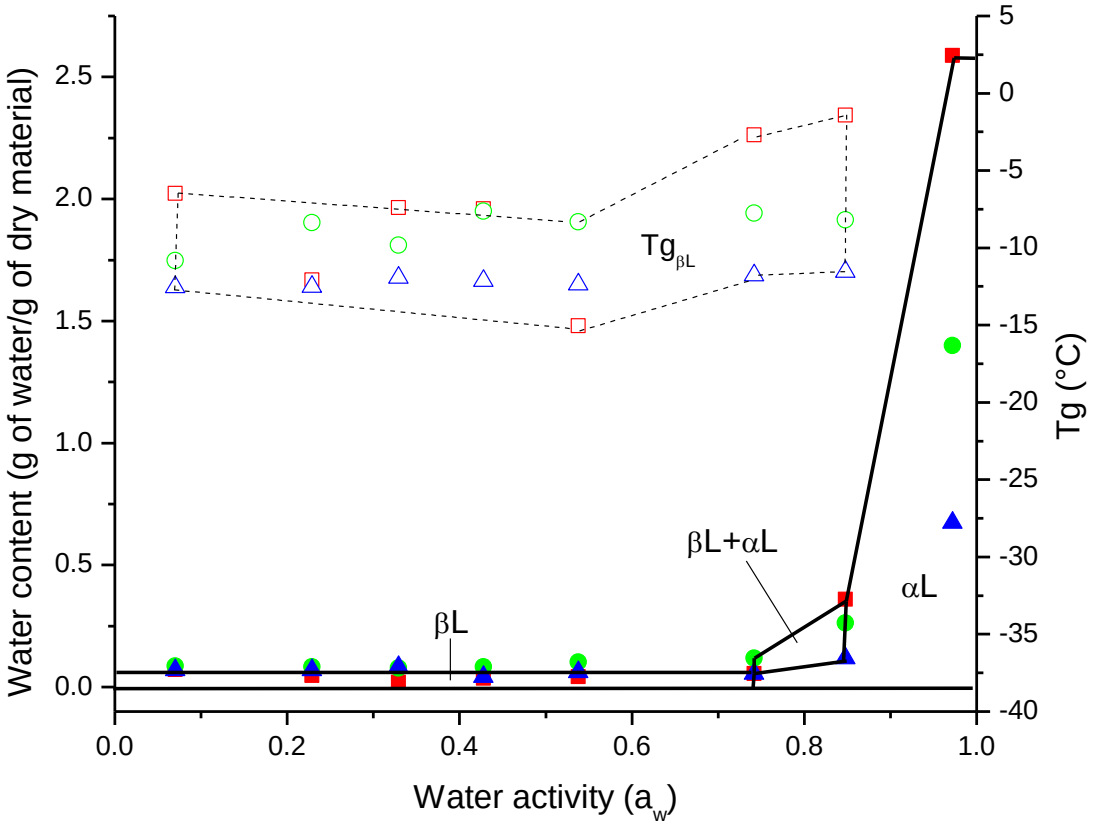


Fig. 6. Equilibrium state diagram of Lβ in the water activity range of 0.07-0.972 at storage temperatures. The continuous line indicates the limits of stability, while the dashed line encloses the Tg values of Lβ. Filled square (■), circle (●) and triangle (▲) indicate the water content at temperatures of 15, 25 and 35 °C, respectively. Open square (□), circle (○) and triangle (△), correspond to the Tg values determined at temperatures of 15, 25 and 35 °C.

Table 1. GAB parameter of Lβ isotherms at different temperatures.

Parameter	Temperature		
	15 °C	**25 °C**	**35 °C**
Xm	0.0387	0.0409	0.0219
C	38098.75	38093.75	38093.75
K	1.0187	0.9987	0.9953
R^2	0.986	0.994	0.995

Table 2. Summary of the Tg values of Lβ at the different storage conditions.

	15 °C			25 °C			35 °C		
Aw	Initial	Middle	End	Initial	Middle	End	Initial	Middle	End
0.07	-7.91	-6.47	3.86	-14.29	-10.82	4.43	-17.3	-12.55	-8.14
0.229	-13.91	-12.09	-1.55	-13.25	-8.36	5.96	-14.5	-12.51	-10.48
0.329	-8.65	-7.41	-0.84	-16.88	-9.84	8.57	-14.15	-11.93	-4.31
0.428	-14.94	-7.49	2.42	-13.52	-7.64	-1.46	-13.88	-12.14	-3.91
0.538	-18.51	-15.05	-11.35	-11.8	-8.33	-0.69	-15.92	-12.37	-5.78
0.742	-8.01	-2.69	5.14	-15.54	-7.76	3.1	-14.08	-11.78	-4.01
0.848	-9.01	-1.43	9.51	-13.12	-8.2	-4.69	-14.2	-11.54	-2.58
0.848*	84.26	86.85	87.19	77.27	80.34	83.31	77.21	81.33	86.24
0.972	------	-----	-----	-----	-----	-----	-----	-----	------
0.972*	73.91	80.41	88.01	78.35	81.15	87.30	75.69	79.81	90.56

*Tg α-Lactose